



ORIGINAL ARTICLE

Industrial indigo dyeing wastewater purification: Effective COD removal with peroxi-AC electrocoagulation system



Wei Zhang^{a,b,*}, Mengdi Zhang^a, Jiming Yao^a, Jiajie Long^{b,c}

^a College of Textile and Garments, Hebei University of Science and Technology, Shijiazhuang 050000, China

^b Jiangsu Engineering Research Center of Textile Dyeing and Printing for Energy Conservation, Discharge Reduction and Cleaner Production (ERC), Soochow University, Suzhou 215123, China

^c College of Textile and Clothing Engineering, Soochow University, Suzhou 215123, China

Received 25 September 2022; accepted 15 January 2023

Available online 24 January 2023

KEYWORDS

Indigo dyeing wastewater;
Electrocoagulation;
Alternating/direct current;
Fenton reaction;
COD removal

Abstract Direct current (DC) electrocoagulation has obvious decolorization effect on indigo dyeing wastewater produced in actual production, while the removal rate of chemical oxygen demand (COD) was less than 40%, accompanied by serious electrode corrosion and high energy consumption. In order to enhance the COD removal rate, reduce the electrode loss and power consumption, a peroxi-alternating current (AC) electrocoagulation (EC) system was constructed. With COD as the main evaluation index, the effects of power type, electrode combination and process parameters on COD removal rate and decolorization rate were focused on and explored, as well as revealing the degradation mechanism of COD. The results showed that AC electrocoagulation enhanced the floc adsorption capacity by improving the floc structure, and the COD removal rate after treatment was 51.19%. The coupled system of peroxi-AC electrocoagulation further removed sulfite and residual dyes in the wastewater, and the COD removal and decolorization rate of the treated wastewater reached 78.09% and 98.47%, respectively. In addition, the specific energy consumption analysis of COD removal showed that the coupled system was far less energetic than the DC electrocoagulation process, with only 30% of its energy consumption. The uniform corrosion of the electrode under the action of AC weakened the passivation, which reduced the electrode loss and power consumption by 22.73% and 43.75%, respectively. Results from the present work indicated that the peroxi-AC EC system could be an effective method for reducing the concentration of COD in

* Corresponding author at: Institution: College of Textile and Garments, Hebei University of Science and Technology, NO.26 Yuxiang Street, Yuhua District, Shijiazhuang 050018, China.

E-mail addresses: weizhang2999@163.com, weizhang@hebust.edu.cn (W. Zhang).

Peer review under responsibility of King Saud University.



indigo dyeing wastewater.

© 2023 The Author(s). Published by Elsevier B.V. on behalf of King Saud University. This is an open access article under the CC BY-NC-ND license (<http://creativecommons.org/licenses/by-nc-nd/4.0/>).

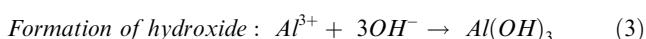
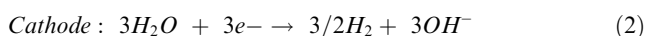
1. Introduction

Indigo, an insoluble dye in water, is a significant vat dye that is widely used in denim dyeing (Zhu et al., 2022). It must be reduced to water-soluble form with an excess of reducing agent under alkaline conditions (pH 11–14) in order to implement the leuco-dyeing process (Saikhao et al., 2018). Sodium dithionite ($\text{Na}_2\text{S}_2\text{O}_4$) is the preferred reducing agent in the industrial dyeing process because it is effective in the successful and rapid reduction of indigo. However, by-products (especially sulfite and sulfate ions) are generated from the reaction of $\text{Na}_2\text{S}_2\text{O}_4$ (Hendaoui et al., 2021, Li et al., 2020). It is estimated that about 10–30 % of the dyes are unfixed and are discharged into the wastewater (Chowdhury et al., 2020). Thus, the indigo dyeing wastewater is characterized by dark color, high alkalinity and COD value.

Indigo dyes are hazardous to human health, causing severe irritation in contact with human skin or eyes, and are carcinogenic to some extent. When entering water bodies, indigo dyes cause the death of aquatic organisms, thus posing a threat to aquatic ecology. Therefore, effective treatment of indigo wastewater is very important to protect the environment. The biodegradability of indigo dyeing wastewater is very low. The biological technique alone is very inefficient and requires long treatment times. Buscio et al. used polyvinylidene difluoride ultrafiltration membranes to treat wastewater containing indigo dye. The COD and dye removal obtained was 67 % and 98 %, respectively (Buscio et al., 2015). Ahmed et al. prepared a layered double hydroxide by sol–gel route for the removal of indigo carmine dye. They found that the maximum adsorption of the dye was over 95 % (Ahmed et al., 2017). AbouSeada et al. used a synthetic magnetic ferric cobalt chloride/tin oxide ($\text{CoFe}_2\text{O}_4/\text{SnO}_2$) nanoparticle for photodegradation of indigo carmine dye. Although the addition of CoFe_2O_4 reduced the band gap energy and facilitated the recovery of the catalyst, it also hindered the metallic properties of the active site of SnO_2 particles and reduced the catalytic efficiency, resulting in less than 55 % dye removal efficiency (AbouSeada et al., 2022). However, these methods are very expensive to use and maintain, and they limit the large-scale application in factories.

Electrocoagulation (EC) was successfully applied to treat dyeing wastewater as an ecofriendly and cost-effective process (Huangfu et al., 2021). There are many inherent advantages compared to other well-known physicochemical treatments in this technique, since its low cost, wide range of application and effectiveness (Donneys-Victoria et al., 2020). In the EC process, the flocculant is generated in situ by electrolytic oxidation of the sacrificial anode. The direct and indirect oxidation present in the system provide additional benefits (Tanveer et al., 2022). Among the different sacrificial anodes have been reported, the inexpensive aluminum and iron are the most commonly used for effluent decontamination (Merma et al., 2020). The summarized reactions are shown as follows.

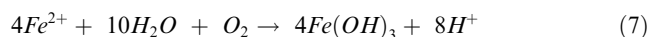
Using aluminum electrodes:



Using iron electrode:

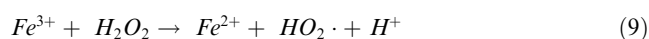
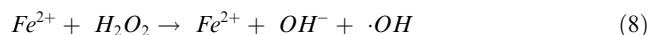


Formation of hydroxide:



The majority of the report on EC is usually powered by a direct current (DC) power supply. However, in the case of DC, the chemical deposits and impermeable dense oxide layers formed on the electrodes would lead to electrode passivation, resulting in a decrease in the efficiency of electrocoagulation (Karamati-Niaragh et al., 2019). In addition, severe anode corrosion shortens the electrode life. The alternating current (AC) power supply was found to effectively improve the treatment efficiency while reducing energy consumption (Mansoorian et al., 2014). Xu et al. compared the removal efficiency and power consumption of DC/AC power supply on the removal of Cu^{2+} from printed circuit board wastewater. The results showed that the removal rates of the power supply to Cu^{2+} reached 98.21 % and 99.86 %, respectively, while the power consumption was $4.42 \times 10^{-2} \text{ kWh}\cdot\text{m}^{-3}$ and $2.76 \times 10^{-2} \text{ kWh}\cdot\text{m}^{-3}$, respectively (Xu et al., 2020). Arabameri et al. also compared the removal efficiency, electrode and power consumption of heavy metal nickel (Ni) by DC and AC power sources. The statistical analysis revealed that the average amount of the remaining nickel was 44.06 and 43.91 $\text{mg}\cdot\text{L}^{-1}$, both power sources could remove heavy metals well. The power consumption and electrode consumption using AC power were 7.47 $\text{kWh}\cdot\text{m}^{-3}$ and 3.07 $\text{kg}\cdot\text{m}^{-3}$, respectively, while the consumption when using DC power were much higher than AC, which were 8.93 $\text{kWh}\cdot\text{m}^{-3}$ and 5.88 $\text{kg}\cdot\text{m}^{-3}$, respectively (Arabameri et al., 2022).

Although the use of AC power can reduce consumption, it provides limited improvement in treatment efficiency. At present, researchers generally use EC together with other treatment technologies (GilPavas et al., 2020, Abdulrazzaq et al., 2021, Zazoua et al., 2019). Sorayyaei et al. successfully applied a combined electrocoagulation-adsorption process for the removal of methyl orange from the aqueous solution, with a dye removal yield of 93.1 % at an adsorbent dosage of 1 g and a voltage of 40 V. However, the high energy consumption limited the continued improvement of efficiency (Sorayyaei et al., 2021). Ravadeli et al. used an electrocoagulation-assisted anoxic/anoxic membrane bioreactor to treat wastewater containing azo dye, which achieved high dye removal efficiency (94.9 %) but resulted in membrane contamination (Ravadeli et al., 2021). In addition to these processes, peroxi-electrocoagulation emerges as an efficient and less expensive method (Garcia-Segura et al., 2017). This treatment process with a dual function of oxidation and coagulation which by adding H_2O_2 in combination with EC technology eliminated refractory and toxic pollutants from the wastewater (Yazdanbakhsh et al., 2015). In addition to the electrochemical reactions mentioned above, H_2O_2 undergone a Fenton reaction catalyzed by Fe^{2+} to produce hydroxyl radicals ($\cdot\text{OH}$), were shown in reaction equations 8–9. Hydroxyl radicals are extremely reactive and non-selective that can oxidize many organic compounds.



According to our best knowledge, the EC technique has drawn no comparison between the DC and AC to remove COD from indigo dyeing wastewater. Besides, some research groups have utilized AC to treat wastewater but have not considered using it in combination with other processes. Combining the advantages of AC and union processes, we constructed a peroxi-AC EC system. By comparing the

treatment effects of DC and AC, the energy supply of the system was determined. Then, three electrode combinations using iron and aluminum were discussed and the reasons for the decrease in COD values were analyzed. Finally, several process parameters such as the amount of H_2O_2 , electrolysis time, applied voltage and output frequency in the system were optimized to achieve the maximum COD removal rate.

2. Materials and methods

2.1. Materials

In this investigation, samples from indigo dyeing wastewater were used, which was taken from Xindadong Textile Co. located in Hebei, China. It must be diluted 5 times before used. Otherwise, the current will exceed the rated range due to the high conductivity of the original wastewater. Table 1 showed the indicators for diluted waste water. 30 % hydrogen peroxide (H_2O_2 , AR) was provided by Tianjin Zhengcheng Chemical Co., Ltd (China). Potassium titanium oxalate ($C_4K_2O_9Ti \cdot 2H_2O$, AR) was provided from Shanghai Macklin Biochemical Co., Ltd (China). 1,10-phenanthroline ($C_{12}H_8N_2$) was purchased from Tianjin Yongda Chemical Reagent Co., Ltd (China). Sulfuric acid (H_2SO_4 , 98 %) was supplied from Shijiazhuang Reagent Factory (China). All aluminum plates and iron plates (Al and Fe, 40 mm \times 40 mm \times 1 mm) were purchased from Shanghai Chuxi Industrial Co., Ltd (China). After each run, electrodes were cleaned with wire brush, washed with HCl (10 %) and deionized water and dried in room temperature.

2.2. Electrochemical systems and procedure

The electrochemical cell was composed from a lab-scale mono-compartmental cylindrical glass reactor containing 250 mL diluted wastewater. The electrodes were vertically located in the reactor and fixed at a distance of 3 cm one from another. Current was induced with the DC regulated power supply (RXN-1503, Zhaoxin Electronics Co., Ltd., China) and AC inverter power supply (PW-350, Dongguan Napui Electronics Technology Co., Ltd., China). Three different electrode configurations were employed for EC process. In the first configuration, both electrodes were made of iron (Fe-Fe). For the second configuration, both electrodes were made of aluminum (Al-Al). In the last configuration, iron and aluminum were used as plates (Fe-Al). In the peroxi-AC process, H_2O_2 was added into the EC system to stimulate the Fenton reaction

in the process. In order to maintain the homogeneity, a magnetic stirrer with a speed of 180 rpm was employed. All the runs were performed at room temperature 25 ± 1 °C. A schematic diagram describing the electrochemical process was shown in Fig. 1.

2.3. Analytical methods and characterization

The dye concentration was estimated from its absorbance at the maximum wavelength (670 nm) using UV-visible spectrophotometer (JH756, Shanghai Jinhua Technology Co., Ltd., China). The COD values of the supernatant were determined by COD rapid detector (LY-C3, Qing Dao Lvyu Environmental Protection Technology Co., Ltd., China). In order to remove the influence of Cl^- on COD results, Cl^- screen agent was added during COD test. The decolorization and COD removal efficiencies were calculated as the following equation:

$$R_e = \frac{X_0 - X_t}{X_0} \times 100\% \quad (10)$$

Where, X_0 and X_t represent the dye and COD content of the wastewater at an initial time and after electrolysis time t , respectively.

To measure the redox potential (mV) standardized at 25 °C, we use a redox potentiometer (FLP201B, Dalian Fulang Electronics Co., Ltd., China). For analysis the corrosion of electrodes, the plates were observed using a microscope head (TIPSCOPE, Wuhan Convergence Technology Co., China). The electrochemical corrosion behavior was analyzed using an electrochemical workstation (CHI660E, Shanghai Chenhua Instruments Co., Ltd., China). The concentration of residual H_2O_2 was measured by spectrophotometry with titanium oxalate.

The chemical composition of supernatant was obtained from different analytical techniques, including Ultraviolet-visible spectroscopy (UV, TU-1810, Beijing Pu-Analysis General Instrument Co., Ltd., China), Fourier Transform Infra-Red (FTIR, Nicolet 6700, Thermo-Fisher, USA) and X-ray Diffraction (XRD, D/MAX-2500, Rigaku, Japan). The morphologies of flocs were measured by optical microscope (OM, XP-202E, Shanghai Bimu Instruments Co., Ltd, China) plus scanning electronic microscopy (SEM, TM-3000, Hitachi, Japan). The surface area of flocculent precipitates was determined by Brunauer-Emmet-Teller (BET) method and pore volume (ASAP2460, Micromeritics, USA).

3. Results and discussion

3.1. EC process

3.1.1. Effect of power supply type

Different current waveforms of the power supply have a direct effect on electrode corrosion. Herein, the DC and AC power supply were applied, and the wastewater was electrolyzed at a voltage of 20 V for 40 min. The morphology of the electrode surface after electrolysis (DC and AC) which shown in Fig. 2. The corrosion gouges distributed deeply on the electrode surface during DC treatment. In contrast, for the electrodes treated under AC, fewer disordered shallow pits were formed (Ingelsson et al., 2020). It indicated that the dissolution of the electrodes was more uniform due to the cyclic transition

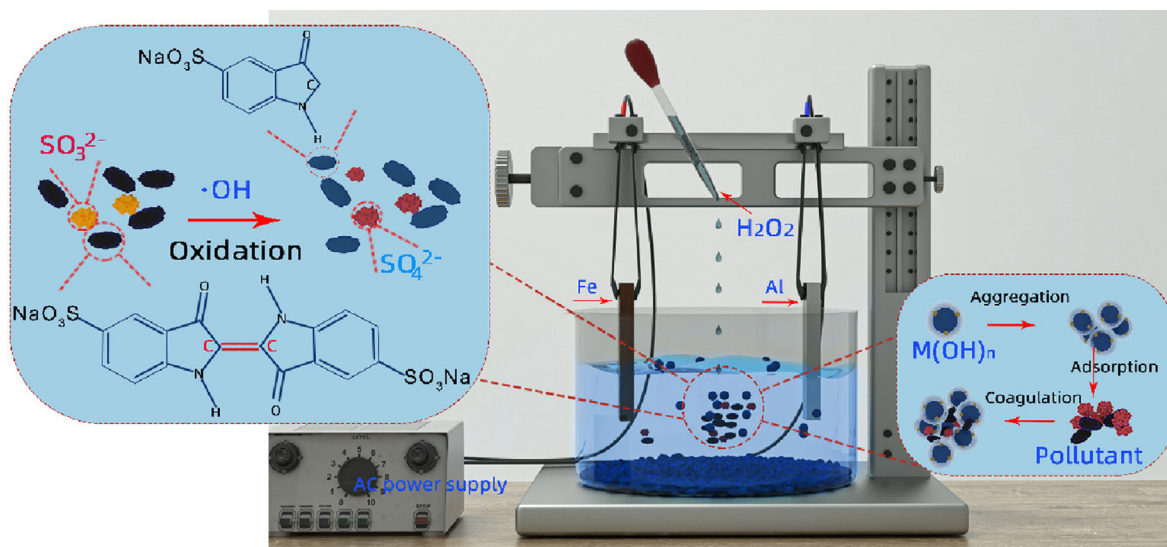
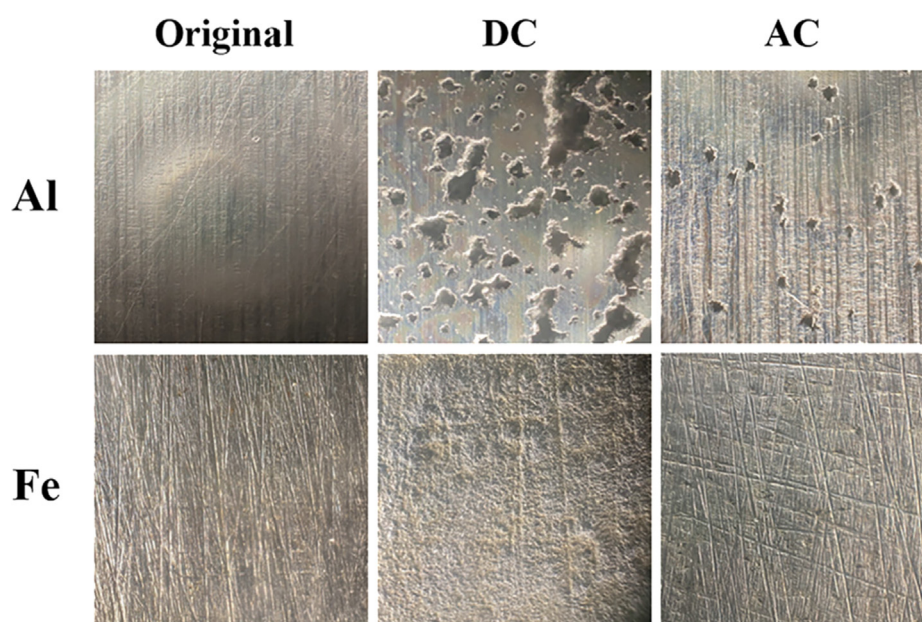
Table 1 Characteristics of diluted indigo dyeing wastewater.

Parameter	Value	Permissible limit
COD (mg/L)	538.2	200
pH	9.55	6 ~ 9
Color (Pt-Co)	400	80
Electrical conductivity (mS/cm)	4.63	–
redox potential (mV)	–420	–
Absorbance (670 nm)	2.281	–
Turbidity (FTU)	120	–
Total solids (g/L)	2.26	–
Appearance	Blue	–

The permissible limits were issued by the Ministry of Environmental Protection, PRC on October 19, 2012.

Table 2 Indicators after DC and AC.

Power Type	DC		AC		
	Al	Fe	Al-Al	Fe-Fe	Fe-Al
Decolorization rate (%)	93.66	86.84	96.68	90.42	95.32
COD removal rate (%)	40.66	29.41	48.69	36.23	51.19
Electrode loss rate (%)	10.94	2.75	3.62	0.62	1.68
Power consumption (kW-h)	16.22×10^{-3}	18.14×10^{-3}	10.36×10^{-3}	12.04×10^{-3}	12.14×10^{-3}
Precipitates mass (g)	0.38	0.40	0.28	0.29	0.29

**Fig. 1** Electrochemical experimental device and experimental reaction principle.**Fig. 2** Photos of electrodes (corrosion Al and Fe) by DC and AC ($\times 400$).

of the current. As shown in [Table 2](#), AC power resulted in less electrode loss and power consumption, as well as less flocs generated, and the decolorization and COD removal rates were improved. In order to build the low consumption and high efficiency electrochemical system, AC power supply was chosen.

3.1.2. Polarization curves

The corrosion of the electrodes was further analyzed by the polarization curves ([Fig. 3](#)). The characteristics of the polarization curves obtained for the Al electrode by DC and AC power

were similar. Combined with the microscopic observation of the electrode corrosion, it was evident that the corrosion was point corrosion. Point corrosion was localized corrosion in the shape of small holes formed on the surface of the electrode, where the electrode was deeply corroded along the location of the small holes. For the Fe electrode, there was an obvious passivation interval (-0.354 ~ -0.107 V) after DC treatment, while it was not observed after AC treatment. Furthermore, the self-corrosion potentials of Al and Fe electrodes were -0.56 V and -0.59 V under the power of DC. And the value was both -0.61 V with the condition of AC. The negative shift of the self-corrosion potentials indicated that AC could inhibit passivation and activate the electrodes.

3.1.3. Characterization of the flocculent precipitates

Theoretically, the more flocs produced, the more pollutants will be adsorbed (Lu et al., 2022). In the above experimental, decolorization and COD removal was better under AC conditions, but the precipitates mass was smaller instead. Consequently, the structures of the precipitates produced under DC and AC were further analyzed. An aqueous solution with C_{NaCl} of $1 \text{ g}\cdot\text{L}^{-1}$ was configured for the experiment in order to obtain the flocs without adsorption of pollutants. The flocs were formed by electrolysis at pH 7 and applying 20 V for 40 min by DC and AC, respectively. Optical micrographs of the flocculent precipitates were shown in Fig. 4 (a). The flocculent precipitates of irregular small lamellae had good light transmission were formed under DC conditions. The AC mode produced large and opaque sediment particles. This indicated that the three-dimensional structure of the flocs produced under AC conditions was more integrity.

In general, high specific surface area and large pore volume are more favorable for adsorption (Long et al., 2021). The physical structure of the flocculent precipitates was measured by nitrogen (N_2) adsorption-desorption using a surface area analyzer, and the results were shown in Fig. 4 (b). Since both have hysteresis loops, they conform to the type IV adsorption isotherms prescribed by IUPAC and the flocculent particles

generated under DC and AC conditions were mesoporous materials (Thommes et al., 2015). As could be seen from Fig. 4 (c), the mesopores generated under DC had a pore size of approximately 3 nm, while those generated under AC were about 10 nm. The mesopores generated under AC were much larger than those under DC. According to BET specific surface area analysis (Table 3), the specific surface areas of the precipitates produced under the two powers were about $308.37 \text{ m}^2\cdot\text{g}^{-1}$ and $316.40 \text{ m}^2\cdot\text{g}^{-1}$, while the pore volume of precipitates produced by AC was almost twice as large as that of DC. In summary, the AC power supply resulted in enhanced adsorption properties of the flocs.

3.2. Peroxi-AC electrocoagulation

The peroxi-electrocoagulation is an emergent technology can simultaneously generate hydroxyl ($\cdot\text{OH}$) and other chemical oxidants through different mechanisms. These highly oxidant species improve the removal of pollutants due to (i) the acceleration of anodes dissolution by chemical oxidation and (ii) enhancement of the pollutants' abatement via the oxidation action of radical species (Vale-Júnior et al., 2018). A peroxi-AC electrocoagulation (hereafter abbreviated as peroxi-AC EC) system was constructed by adding H_2O_2 and using Al and Fe as electrodes, powered by an AC power supply.

3.2.1. Effect of electrode combination

The decolorization and COD removal rates of the supernatants after the reaction with three electrode combinations ((I) Al-Al; (II) Fe-Fe; and (III) Fe-Al) were shown in Fig. 5 (a) and (b). It could be seen that the best decolorization and COD removal results were obtained using the Fe-Al electrode combination. It is noteworthy that compared with the Al-Al electrode, the Fe-Fe electrode possessed lower decolorization rate but higher COD removal rate. This is because the Fe^{2+} could catalyze the decomposition of H_2O_2 to produce more $\cdot\text{OH}$ to oxidize pollutants.

The SEM images of the flocculent precipitates were shown in Fig. 5 (c). The surface morphology of the precipitates from the Fe-Al electrode was rougher and more porous with uneven surface, which was more conducive to the adsorption compared to other electrode combinations. Therefore, the improvement in the removal efficiency with Fe-Al electrode could be attributed to two aspects: catalytic effect of the Fe electrode, and the higher surface area and available adsorption sites of the flocs. In the combination of Fe-Al electrodes, more flocs with adsorption were created than in the condition of Fe-Fe electrodes, due to the presence of Al, resulting in a higher decolorization rate. The Fe allowed more free radicals to be produced in the system than that in the system of the Al-Al electrodes, resulting in better COD removal. To enhance the removal of pollutants, a combination of Fe and Al electrodes was selected.

3.2.2. The mechanism of COD removal

Biodegradable organic compounds, non-biodegradable compounds and inorganic oxidizable compounds contribute to COD in wastewater (Moreno-Casillas et al., 2007). The UV spectra of the supernatants was shown in Fig. 6 (a). The peaks observed in the visible region (around 670 nm) and the UV region (around 291 nm, 347 nm) were the characteristic peaks

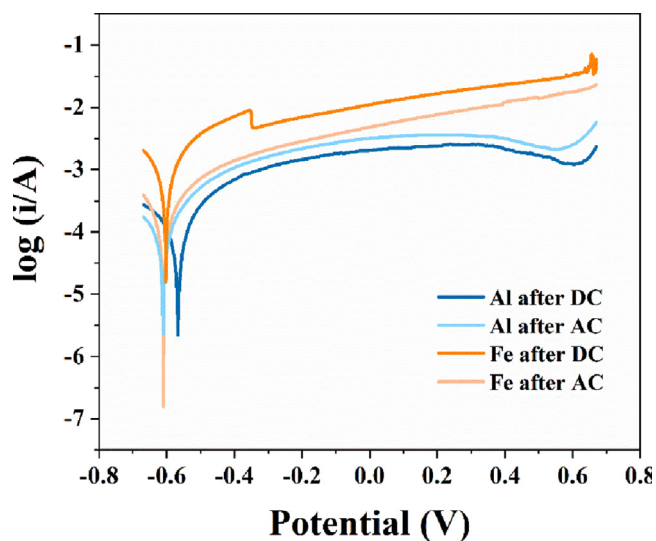


Fig. 3 Polarization curves of Al and Fe electrodes after DC and AC treatment.

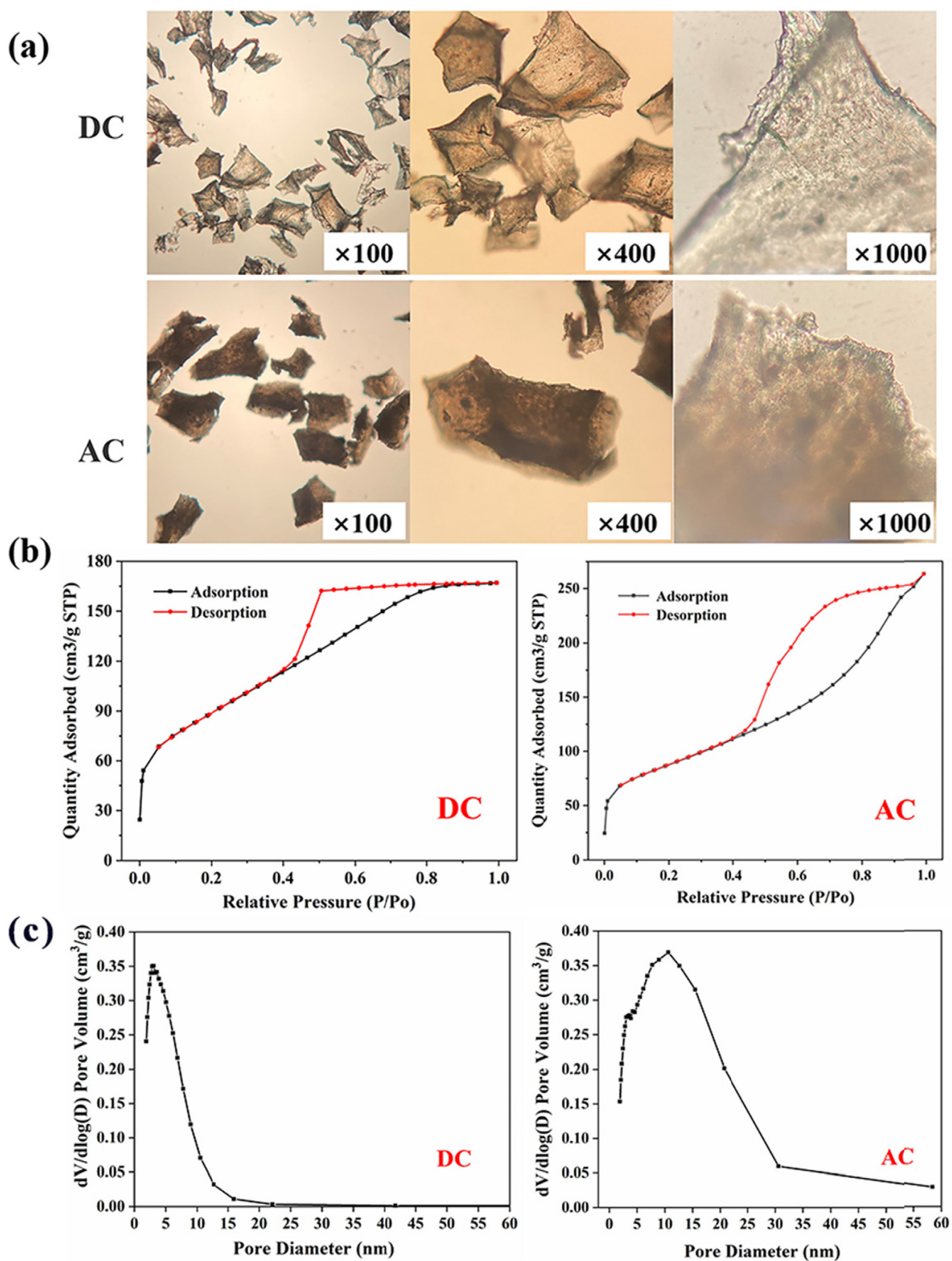


Fig. 4 (a) Microscopic observation of flocculent precipitates; (b) N_2 adsorption–desorption isotherms for samples: DC (left), AC (right); (c) The distribution of mesopore: DC (left), AC (right).

Table 3 Physical structure parameters of flocculent precipitates.

Power Type	Specific surface area ($\text{m}^2\cdot\text{g}^{-1}$)	Pore volume ($\text{cm}^3\cdot\text{g}^{-1}$)	Average aperture (nm)
DC	308.3682	0.2583	3.6699
AC	316.4008	0.4061	6.1786

of indigo dye. The disappearance of the characteristic peaks after the EC and peroxi-AC EC indicated that the insoluble indigo dye was completely removed.

The soluble inorganic matter in the solution also affects the COD values. The FT-IR spectra characteristic peaks at 980–910 and 660–615 cm^{-1} were SO_3^{2-} , while the peaks at 680–580 and 1210–1040 cm^{-1} attributed to SO_4^{2-} (Besharatlou et al., 2021, Hevira et al., 2020). As shown in Fig. 6 (b), the peak near 966.3 cm^{-1} belonging to SO_3^{2-} largely disappeared after the peroxi-AC EC. This implied that it may be oxidized to SO_4^{2-} . The phenomenon was verified by XRD analysis (Fig. 6 (c)), where sulfite and sulfate structures were presented in both the original wastewater and the supernatant after EC, while dissolved sulfite was removed or oxidized through

peroxi-AC EC. Taken together, indigo wastewater treated with peroxi-AC EC effectively removed not only dyes but also sulfites.

3.3. Optimization of peroxi-AC EC system

The peroxi-AC EC system was further optimized to achieve good COD removal and ensure the full utilization of H_2O_2 . The effects of four factors on the system, namely the amount of hydrogen peroxide, electrolysis time, applied voltage and output frequency were selected and discussed.

3.3.1. Effect of H_2O_2 amount

It is important to optimize the amount of H_2O_2 used in the peroxi-AC EC due to cost and the reaction of excess H_2O_2 with $\cdot\text{OH}$ to form less oxidizing hydrogen peroxide radicals ($\text{HO}_2\cdot$) (Venu et al., 2014). Fig. 7 showed the effect of H_2O_2 amount on COD removal rate, H_2O_2 utilization and redox potential when the voltage was 20 V, the electrolytic time was 40 min and the output frequency was 50 Hz. The COD removal rate was increased from 60.22 % to 71.14 % with increasing the amount of H_2O_2 from 0.8 $\text{g}\cdot\text{L}^{-1}$ to 2.4 $\text{g}\cdot\text{L}^{-1}$. Continue to increase the amount, the COD removal rate was decreased as the undecomposed H_2O_2 interfered with the COD measurement. It was noticed that the highest COD

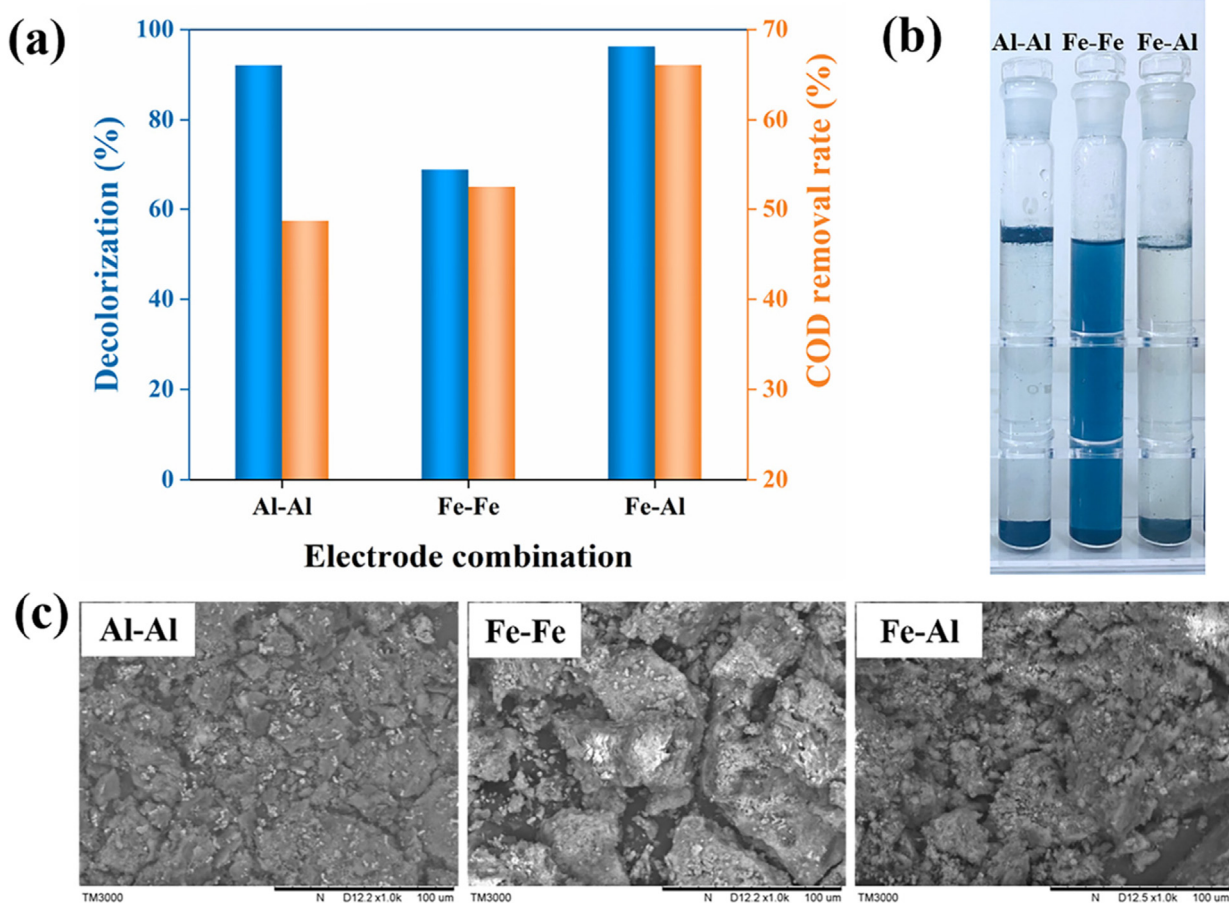


Fig. 5 Effect of electrode combination: (a) on decolorization rate and COD removal; (b) on supernatants; (c) on flocculent precipitates.

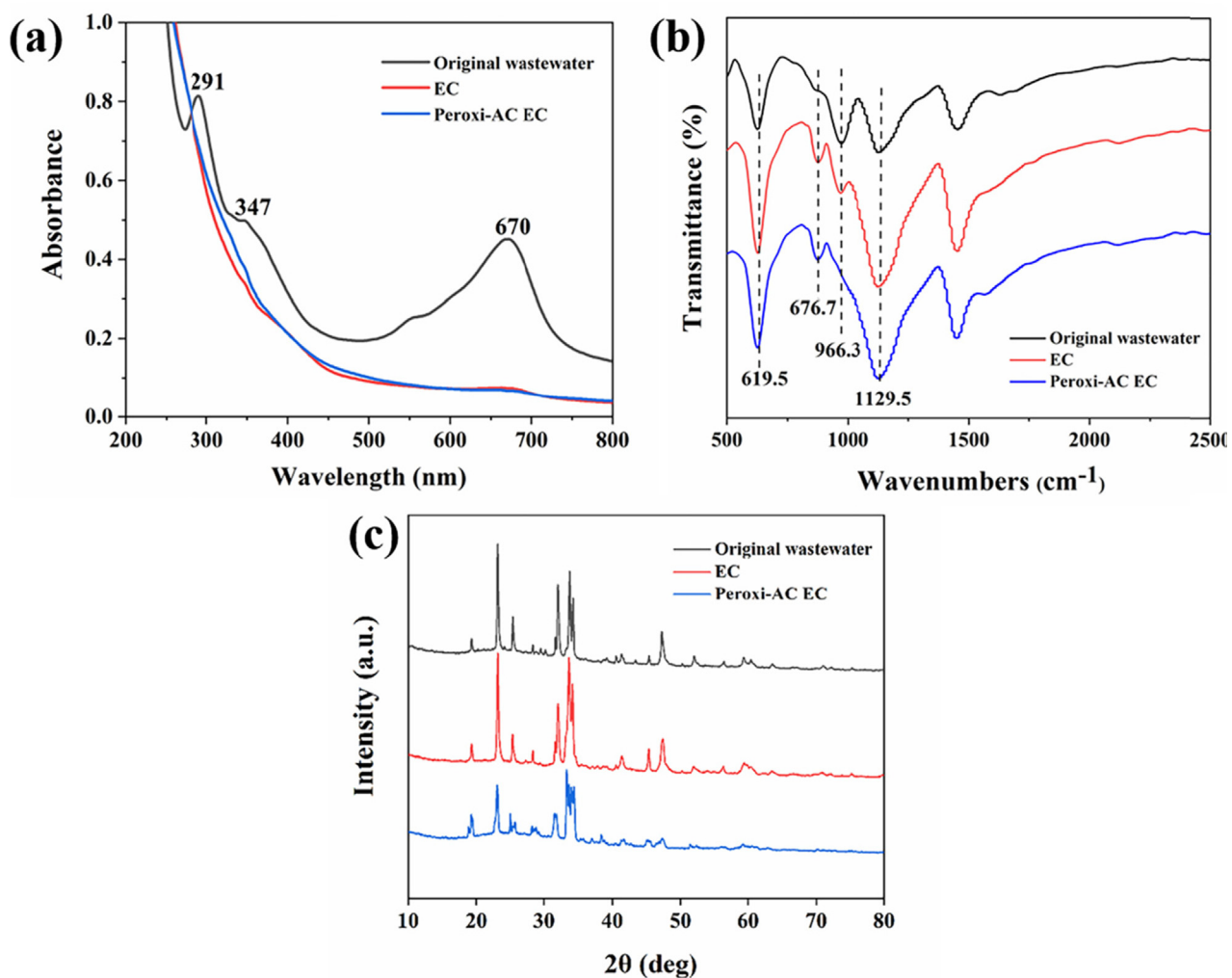


Fig. 6 Analysis of original wastewater and treated supernatant: (a) UV spectra, (b) FT-IR spectra, (c) XRD spectra.

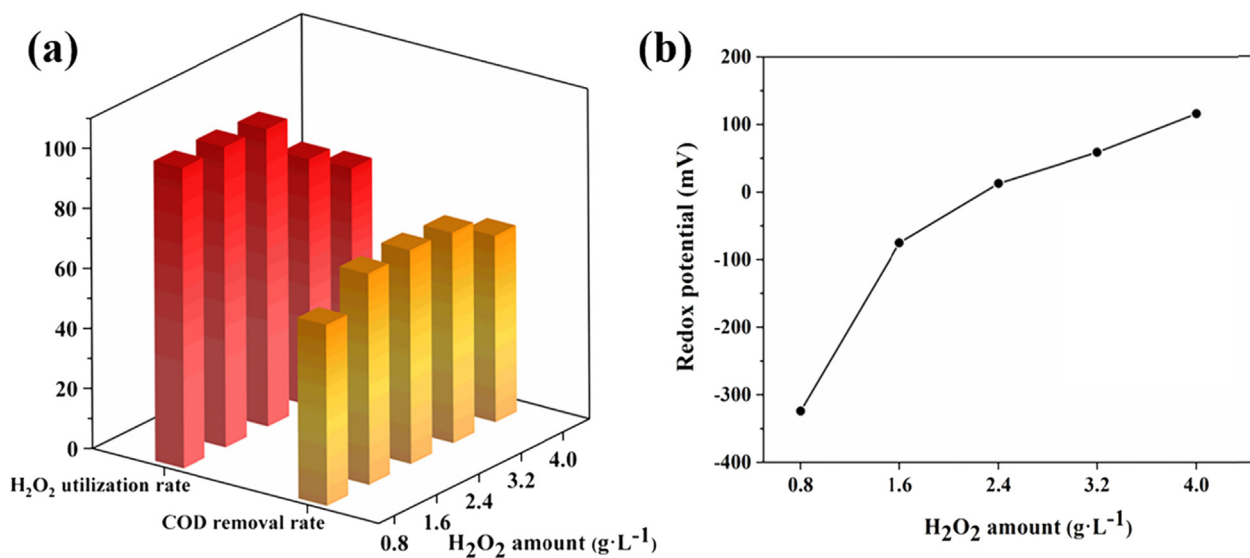


Fig. 7 Effect of H_2O_2 amount: (a) on COD removal and H_2O_2 utilization; (b) on redox potential.

removal was obtained at the redox potential close to the zero point, when there was no H_2O_2 remained. Therefore, solution the reducing or oxidizing substances also had a significant effect on COD value. In order to achieve high COD removal and ensure the complete decomposition of H_2O_2 , the amount should preferably be around $2.4 \text{ g}\cdot\text{L}^{-1}$.

3.3.2. Effect of electrolysis time

Electrolysis time is effective in generating flocs and hydroxyl radicals (Sanni et al., 2022). The treatment effectiveness of wastewater was evaluated by COD removal and decolorization rate, and the presence of oxidizing or reducing substances in the solution could be monitored by redox potential. The effect results of electrolysis time at a voltage of 20 V, an H_2O_2 dosage of $2.4 \text{ g}\cdot\text{L}^{-1}$ and an output frequency of 50 Hz were shown in Fig. 8. The decolorization rate was increased to 98 % when the electrolysis time was increased from 20 to 40 min, and there was no significant improvement when the time was further extended. Theoretically the COD removal rate should increase gradually with the decomposition of H_2O_2 , but it showed a decreasing trend when the electrolysis time exceeded 40 min. At this time, the redox potential was negative values, indicating the presence of reducing ions in the solution, which were monitored as ferrous ions (Fe^{2+}) after detection. The free ferrous ions were reductive and the more negative the redox potential after the reaction, the more ferrous ions remained. Due to its interference, the COD removal rate decreased. In summary, the electrolysis time was set to 40 min in order to avoid the generation of Fe^{2+} by prolonged electrolysis.

3.3.3. Effect of applied voltage

The higher the current density, the faster the reaction rate (Özyonar et al., 2022). Voltage is positively correlated with current density, and the increasing of the voltage is benefit for enhancing the COD removal and decolorization. The effect results of applied voltage at an H_2O_2 amount of $2.4 \text{ g}\cdot\text{L}^{-1}$, an electrolysis time of 40 min and an output frequency of 50 Hz were shown in Fig. 9. The increase of voltage improved the decomposition efficiency of H_2O_2 , so that both COD removal

and decolorization rates gradually increased, while the redox potential tended to decrease. When the voltage was 20 V, the COD removal rate reached 78.09 %. Above 20 V, the redox potential was observed to become negative, at which time the COD removal rate was decreased by Fe^{2+} . The higher voltage was beneficial, but the suitable applied voltage should be controlled at 20 V.

3.3.4. Effect of output frequency

During the application of AC, the constantly switching positive and negative electrodes reciprocate the flow of ions in the reactor in both directions, resulting in well-mixing solution (Weisbart et al., 2020). Under the conditions of voltage of 20 V, H_2O_2 amount of $2.4 \text{ g}\cdot\text{L}^{-1}$ and electrolytic time of 40 min, the effects of different frequencies were shown in Fig. 10. The peak values of COD removal and decolorization rates were obtained at 50 and 60 Hz. The redox potential changed in an opposite trend with a “W” shape. This was due to the fact that the electrolysis time was set to 40 min (i.e., 2400 s), so the current underwent a complete AC cycle when the frequency was 50 and 60 Hz. The used of AC power should pay attention to both frequency and time to ensure the cycle was complete. The increase in frequency leads to useless loss of energy (Dacic et al., 2021). In order to save electric energy, the output frequency was selected as 50 Hz. At this frequency, the COD and color removal rates were 78.09 % and 98.47 %, respectively. The COD value after treatment at this point was calculated to be 117.92 mg/L, which was far below the permissible limit (shown in Table 1).

3.4. Specific energy consumption analysis

Electrode loss and power consumption are the main costs in the electrocoagulation process, and sludge is the main waste source. The SEC for COD removal could be found from the power consumption and the COD removal rate. The calculation equation was shown below.

$$SEC = \frac{UIt}{V\Delta COD} \quad (11)$$

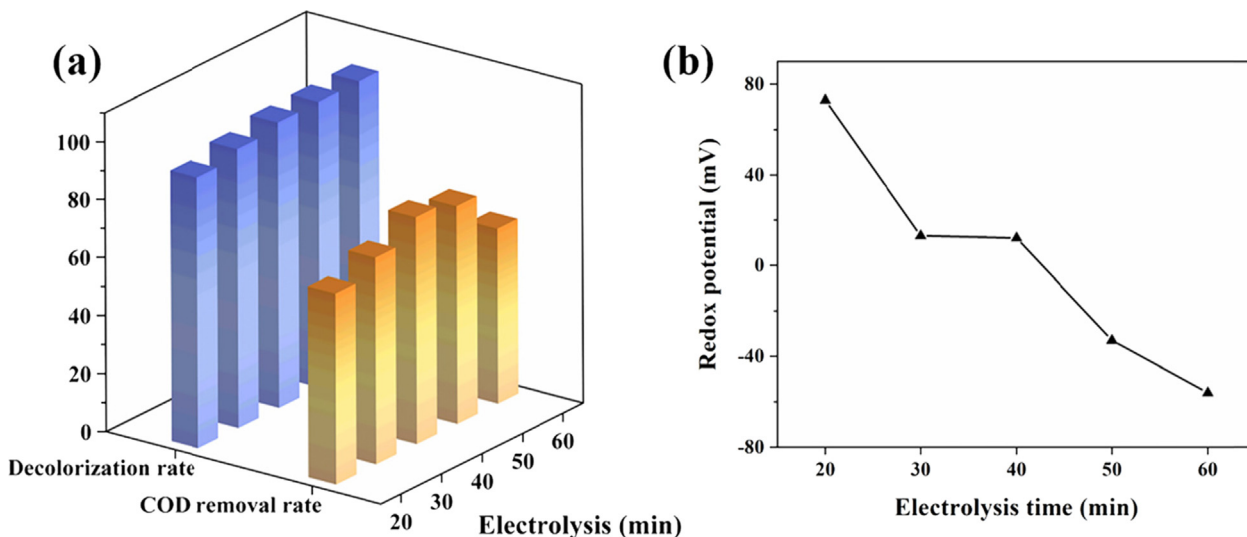


Fig. 8 Effect of electrolysis time: (a) on COD removal and decolorization; (b) on redox potential.

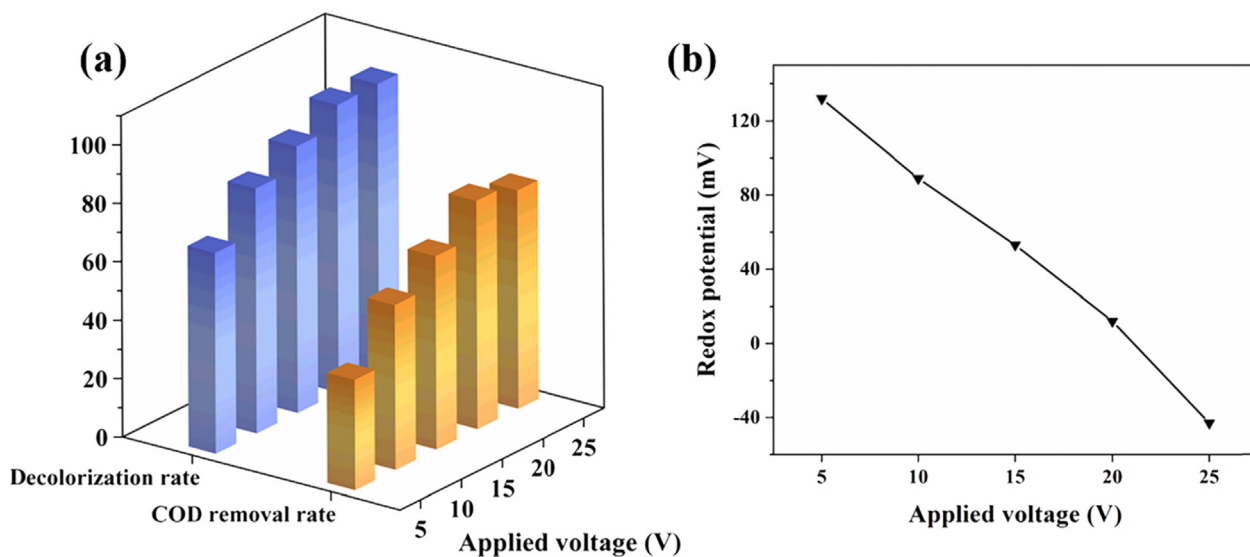


Fig. 9 Effect of applied voltage: (a) on COD removal and decolorization; (b) on redox potential.

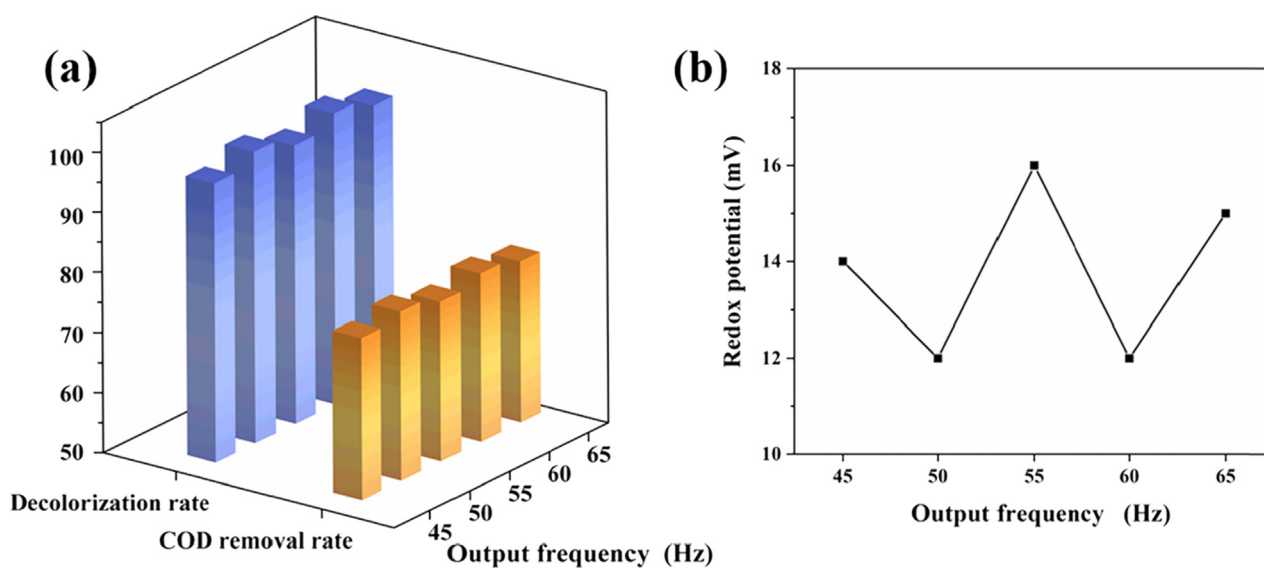


Fig. 10 Effect of output frequency: (a) on COD removal and decolorization; (b) on redox potential.

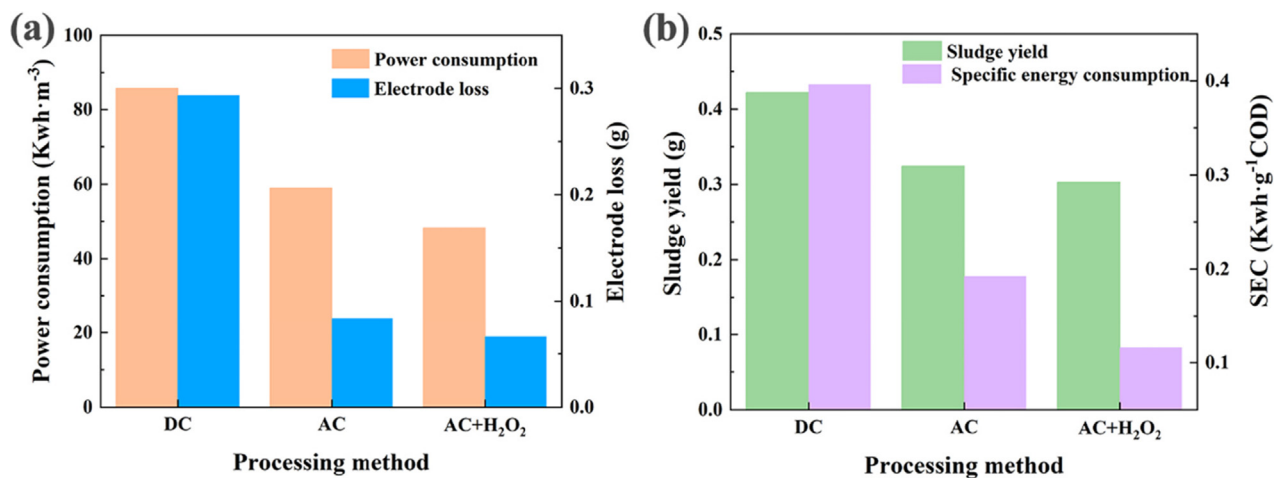


Fig. 11 Different processing methods of: (a) power consumption and electrode loss; (b) sludge production and SEC for COD removal.

Where, *SEC* is the specific energy consumption (kWh/g COD), *U* represents the applied voltage (V), *I* represents the current intensity (A), *t* represents the reaction time (h), *V* represents the treated wastewater volume (L), and Δ COD represents the difference of chemical oxygen demand (g COD/L).

As shown in Fig. 11 (a), the optimized peroxi-AC EC system not only substantially reduced the power consumption under AC conditions, but also greatly decreased the electrode loss (by 43.75 % and 22.73 %, respectively). Furthermore, according to 11 (b), the production of sludge was significantly reduced. Most importantly, the *SEC* of the peroxi-AC EC system was extremely low, i.e., the process made full use of electrical energy to achieve higher pollution removal. The *SEC* of the coupled system for COD removal was only 30 % of that of DC electrocoagulation, and the sludge yield and *SEC* were 0.30 g and 0.12 kWh/g COD, respectively. The above analysis only considered the electrical energy consumption and did not include the consumption of H₂O₂. Although the addition of H₂O₂ resulted in a slightly higher cost, the better removal efficiency meant that many subsequent treatment steps could be eliminated, effectively shortening the full treatment process.

4. Conclusion

The present findings confirm that peroxi-AC EC is a quiet effective method to remove dye and COD from indigo wastewater. The generation of ·OH and flocs with strong adsorption properties was promoted by using a combination of iron and aluminum electrodes. The improvement in COD by this method was attributed to more dye adsorption and soluble inorganics (mainly sulfites) removal. To further boost COD elimination, the effects of H₂O₂ dose, electrolysis time, voltage and frequency were optimized, which showed 78.09 % and 98.47 % of the COD removal and decolorization rates, respectively. The subsequent investigation of the pole plate spacing, initial pH and other factors were also continued. The least operation cost from the viewpoint of electrodes and energy consumption was achieved in the peroxi-EC process using AC power, the *SEC* of the peroxi- AC EC system for COD removal was reduced by 70 % compared to the DC EC. In addition, the application of AC resulted in flocs with higher adsorption capacity and less sludge. These findings demonstrate that the peroxi-AC EC with iron and aluminum electrodes may be successfully employed at an industrial scale to treat real effluent at a reasonable cost and in a short period.

Declaration of Competing Interest

The authors declare no known competing financial interests or personal relationships that could have appeared to affect the study.

Acknowledgment

We acknowledge financial support from the Natural Science Foundation of Hebei Province, China (Grant number: B2022208014), Key Research and Development Program of Hebei Province, China (Grant number: 20374004D), Opening Project of Jiangsu Engineering Research Center of Textile Dyeing and Printing for Energy Conservation, Discharge Reduction and Cleaner Production (ERC), (Grant number: SDGC2105), Fundamental Research Funds for Hebei Universities, China (Grant number: 2021YWF17) and Hebei Province Graduate Student Innovation Funding Project, China (Grant number: CXZZSS2022086).

References

- Abdulrazzaq, N.N., Al-Sabbagh, B.H., Shanshool, H.A., 2021. Coupling of electrocoagulation and microflotation for the removal of textile dyes from aqueous solutions. *J. Water Process Eng.* 40, 101906.
- Abouseada, N., Ahmed, M.A., Elmahgary, M.G., 2022. Synthesis and characterization of novel magnetic nanoparticles for photocatalytic degradation of indigo carmine dye. *Mater. Sci. Energy Technol.* 5, 116–124.
- M.A. Ahmed, A.A. brick, A.A. Mohamed, An efficient adsorption of indigo carmine dye from aqueous solution on mesoporous Mg/Fe layered double hydroxide nanoparticles prepared by controlled sol-gel route, *Chemosphere*, 174 (2017), pp. 280-288
- Arabameri, A., Moghaddam, M.R.A., Azadmehr, A.R., Shabestar, M. P., 2022. Less energy and material consumption in an electrocoagulation system using AC waveform instead of DC for nickel removal: Process optimization through RSM. *Chem. Eng. Process* 174, 108869.
- Besharatlou, S., Anbia, M., Salehi, S., 2021. Optimization of sulfate removal from aqueous media by surfactant-modified layered double hydroxide using response surface methodology. *Mater. Chem. Phys.* 262, 124322.
- Buscio, V., Crespi, M., Gutiérrez-Bouzán, C., 2015. Sustainable dyeing of denim using indigo dye recovered with polyvinylidene difluoride ultrafiltration membranes. *J. Clean. Prod.* 91, 201–207.
- Chowdhury, M.F., Khandaker, S., Sarker, F., Islam, A., Rahman, M. T., Awual, M.R., 2020. Current treatment technologies and mechanisms for removal of indigo carmine dyes from wastewater: a review. *J. Mol. Liq.* 38, 114061.
- Dacic, J., Cheah-Mane, M., Gomis-Bellmunt, O., Prieto-Araujo, E., 2021. Low frequency AC transmission systems for offshore wind power plants: design, optimization and comparison to high voltage AC and high voltage DC. *Int. J. Elec. Power* 133, 107273.
- Donneys-Victoria, D., Marriaga-Cabrales, N., Machuca-Martínez, F., Benavides-Guerrero, J., Cloutier, S.G., 2020. Indigo carmine and chloride ions removal by electrocoagulation. simultaneous production of brucite and layered double hydroxides. *J. Water Process Eng.* 33, 101106.
- García-Segura, S., Eiband, M.M.S.G., Melo, J.V., Martínez-Huitle, C. A., 2017. Electrocoagulation and advanced electrocoagulation processes: a general review about the fundamentals, emerging applications and its association with other technologies. *Electroanal. Chem.* 801, 267–299.
- GilPavas, E., Correa-Sanchez, S., 2020. Assessment of the optimized treatment of indigo-polluted industrial textile wastewater by a sequential electrocoagulation-activated carbon adsorption process. *J. Water Process Eng.* 36, 101306.
- Hendaoui, K., Trabelsi-Ayadi, M., Ayari, F., 2021. Optimization and mechanisms analysis of indigo dye removal using continuous electrocoagulation. *Chinese J. Chem. Eng.* 29, 242–253.
- Hevira, L., Zilfac, R., Ighalo, J.O., Zein, R., 2020. Biosorption of indigo carmine from aqueous solution by Terminalia Catappa Shell. *J. Environ Chem. Eng.* 8, 104290.
- Huangfu, Z.J., Zhang, W., Hao, S., Zhang, M.D., Yao, J.M., 2021. Construction of novel electrochemical treatment systems for indigo wastewater and their performance. *Pigm. Resin Technol.* 50, 264–267.
- Ingelsson, M., Yasri, N., Roberts, E.P.L., 2020. Electrode passivation, faradaic efficiency, and performance enhancement strategies in electrocoagulation—a review. *Water Res.* 187, 116433.
- Karamati-Niaragh, E., Moghaddama, M.R.A., Emamjomeh, M.M., Nazlabadi, E., 2019. Evaluation of direct and alternating current on nitrate removal using a continuous electrocoagulation process: economical and environmental approaches through RSM. *J. Environ. Manage.* 230, 245–254.

- Li, X.Y., Wang, K.K., Wang, M.Q., Yao, J.M., Komarneni, S., 2020. Sustainable electrochemical dyeing of indigo with Fe(III)-based complexes. *J. Clean. Prod.* 276, 123251.
- Long, F.L., Niu, C.G., Tang, N., Guo, H., Li, Z.W., Yang, Y.Y., Lin, L.S., 2021. Highly efficient removal of hexavalent chromium from aqueous solution by calcined Mg/Al-layered double hydroxides/polyaniline composites. *Chem. Eng. J.* 404, 127084.
- Lu, J.C., Zhuo, Q.F., Ren, X.W., Qiu, Y.F., Li, Y.L., Chen, Z.Y., Huang, K.F., 2022. Treatment of wastewater from adhesive-producing industries by electrocoagulation and electrochemical oxidation. *Process Safe. Environ.* 157, 527–536.
- Mansoorian, H.J., Mahvi, A.H., Jafari, A.J., 2014. Removal of lead and zinc from battery industry wastewater using electrocoagulation process: Influence of direct and alternating current by using iron and stainless steel rod electrodes. *Sep. Purif. Technol.* 135, 165–175.
- Merma, A.G., Santos, B.F., Rego, A.S.C., Hacha, R.R., Torem, M.L., 2020. Treatment of oily wastewater from mining industry using electrocoagulation: fundamentals and process optimization. *J. Mater. Res. Technol.* 9, 15164–15176.
- Moreno-Casillas, H.A., Cocke, D.L., Gomes, J.A.G., Morkovsky, P., Pargac, J.R., Peterson, E., 2007. Electrocoagulation mechanism for COD removal. *Sep. Purif. Technol.* 56, 204–211.
- Özyonar, F., Korkmaz, M.U., 2022. Sequential use of the electrocoagulation-electrooxidation processes for domestic wastewater treatment. *Chemosphere* 290, 133172.
- Ravadelli, M., Costa, R.E., Lobo-Recio, M.A., Akaboci, T.R.V., Bassin, J.P., Lapolli, F.R., Belli, T.J., 2021. Anoxic/oxic membrane bioreactor assisted by electrocoagulation for the treatment of azo-dye containing wastewater. *J. Environ. Chem. Eng.* 9, 105286.
- Saikhao et al., 2018. L. Saikhao, J. Setthayanond, T. Karpkird, T. Bechtold, P. Suwanruji. Green reducing agents for indigo dyeing on cotton fabrics, *J. Clean. Prod.* 197 (2018), pp. 106-113.
- Sanni, I., Estahbanati, M.R.K., Carabin, A., Drogui, P., 2022. Coupling electrocoagulation with electro-oxidation for COD and phosphorus removal from industrial container wash water. *Sep. Purif. Technol.* 282, 119992.
- Sorayyaei, S., Raji, F., Rahbar-Kelishami, A., Ashrafzadeh, S.N., 2021. Combination of electrocoagulation and adsorption processes to remove methyl orange from aqueous solution. *Environ. Technol. Inno.* 24, 102018.
- Tanveer, R., Yasar, A., Tabinda, A.-B., Ikhtlaq, A., Nissara, H., Nizami, A.-S., 2022. Comparison of ozonation, Fenton, and photo-Fenton processes for the treatment of textile dye-bath effluents integrated with electrocoagulation. *J. Water Process Eng.* 46, 102547.
- Thommes, M., Kaneko, K., Neimark, A.V., Olivier, J.P., Rodriguez-Reinoso, F., Rouquerol, J., Sing, K.S.W., 2015. Physisorption of gases, with special reference to the evaluation of surface area and pore size distribution (IUPAC Technical Report). *Pure Appl. Chem.* 87, 1051–1069.
- Vale-Júnior, E., Silva, D.R., Fajardo, A.S., Martínez-Huitle, C.A., 2018. Treatment of an azo dye effluent by peroxi-coagulation and its comparison to traditional electrochemical advanced processes. *Chemosphere* 204, 548–555.
- Venu, D., Gandhimathi, R., Nidheesh, P.V., Ramesh, S.T., 2014. Treatment of stabilized landfill leachate using peroxicoagulation process. *Sep. Purif. Technol.* 129, 64–70.
- Weisbart, C., Raghavan, S., Muralidharan, K., Jr, B.G.P., 2020. Feasibility of removal of graphene oxide particles from aqueous suspensions by DC/AC electrocoagulation. *J. Water Process Eng.* 36, 101249.
- Xu, T., Zhou, Y.H., Hu, B.N., Lei, X.P., Yu, G., 2020. Comparison between sinusoidal AC coagulation and conventional DC coagulation in removing Cu²⁺ from printed circuit board wastewater. *Ecotox. Environ. Safe.* 197, 110629.
- Yazdanbakhsh, A.R., Massoudinegad, M.R., Eliasi, S., Mohammadi, A.S., 2015. The influence of operational parameters on reduce of azithromycin COD from wastewater using the peroxi-electrocoagulation process. *J. Water Process Eng.* 6, 51–57.
- Zazoua, H., Afangaa, H., Akhouairi, S., Ouchtak, H., Addi, A.A., Akbour, R.A., Assabbane, A., Douch, J., Elmchaouri, A., Duplay, J., Jada, A., Hamdani, M., 2019. Treatment of textile industry wastewater by electrocoagulation coupled with electrochemical advanced oxidation process. *J. Water Process Eng.* 28, 214–221.
- Zhu, Z., Wan, X., Zhao, S., Liao, Q., Wang, L., Liu, C., 2022. Yi, Foaming indigo: an efficient technology for yarn dyeing. *Dyes Pigments* 197, 109862.